

DC Current Source to Voltage Source CT-Based Converter

DV Nicolae¹⁾, member IEEE and AA Jimoh¹⁾, member IEEE, JFJ van Rensburg²⁾

¹⁾Tshwane University of Technology, Electrical Engineering Department, Pretoria, South Africa

²⁾Vaal University of Technology, Electrical Engineering Department, Vanderbijlpark, South Africa

Abstract: As generally known there is no energy transfer between a dc current and a current transformer. After a brief overview of other methods for tapping energy from the high voltage direct current transmission line, this paper presents the concept of a new dc to ac current source converter utilizing a current transformer. The advantage of this converter is that it is connected in series to the dc line and that at any moment in time the current flow is kept continuous. This paper presents the concept of the converter and simulation results.

I. INTRODUCTION

The power grid is a well-established system for the distribution of electrical energy, but the developing parts of the world tend to remain outside the scope of a typical power system. The issue of small power tapping from high voltage transmission lines in such areas is of great interest. Much has been achieved in tapping from the high voltage alternative current but, in spite of the difficulties, also for the high voltage direct current transmission lines [1-9]. In order to address the problem of HVDC tapping some researchers used hard switching [2, 6, 7, 8] and some other soft switching [9]. In some situations a parallel connection has been proposed [1, 3, 8] but there are also solutions where the converter is series connected [2, 6, 7, 9].

II. OVERVIEW OF DC TAPPING

This class of methods can achieve a relatively high power drawn from the HVDC. These methods are based on power electronics processing of the dc energy transported on the HVDC. There are two possible ways to approach power tapping: in series and in parallel with the line. In this paper only the series connected method will be reviewed as a comparison base for the proposed new series connected method.

A. Current-fed capacitor-switched converter

The basic diagram of this method [6] is presented in Fig. 1. When switches Sw_1 and Sw_3 are ON the capacitor C_1 charges to a voltage proportional to the time current is flowing in it. This voltage is directly applied across the non-conducting switches, as well as the primary of the winding of the air-core isolation transformer. When the voltage reaches a set limit, switches Sw_2 and Sw_4 are triggered thereby naturally commutating Sw_1 and Sw_3 . Now the capacitor C_1 is discharged and charged further in opposite polarity. Thus an alternating voltage of relatively high frequency is created, which is transformed and further processed to the ground

potential. The set voltage limits (V_{c1}) are determined by the switch characteristics [6].

The level of capacitor voltage (V_{c1}) depends directly on the switching frequency. Thus, by varying the switching frequency, the dc bus (V_{dc}) on C_2 can be maintained constant. Fig. 2 shows the steady state for a dc current (I_{dc}) of 2000 A, switching frequency of 830 Hz with a load of 1.4 MVA.

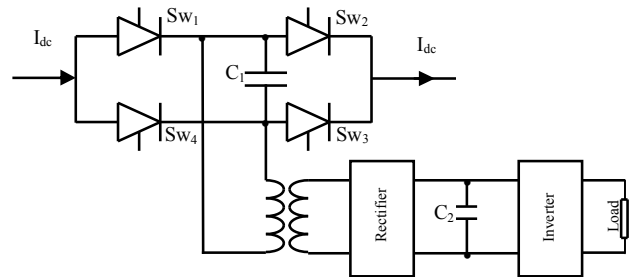


Fig. 1 Current-fed capacitor-switched converter

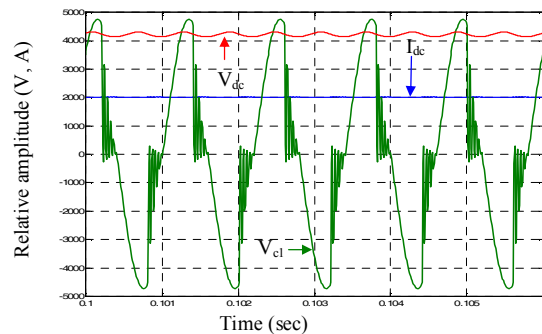


Fig. 2 Steady state for 830 Hz

B. Soft-switch current-fed dc to dc converter

The basic diagram of this tapping method [2] is presented in Fig. 3. It comprise two self-commutated switches (MCT or IGBT) represented by Sw_1 and Sw_2 , two diodes D_1 and D_2 and a snubber capacitor C_H .

The H bridge (Sw_1 , Sw_2 , D_1 and D_2) turns ON at zero current switching conditions and turns OFF at zero voltage conditions. This could contribute to the use of a switching frequency as high as 5 kHz. The alternating voltage created across the primary of the air-core transformer (Tr) is then stepped down and rectified to provide dc voltage (V_{dc}) which can be further used either to supply a dc load or 50 Hz inverter single or three phase.

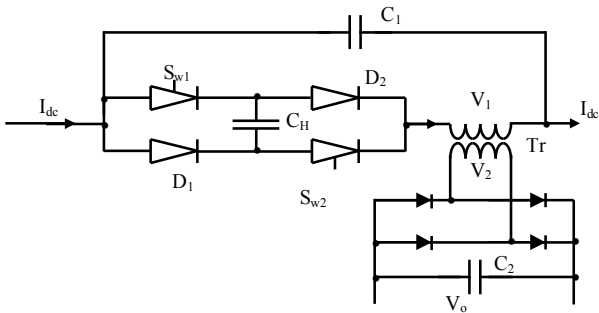


Fig. 3 Soft-switch dc to dc converter

The control of this soft-switching dc/dc converter is based on adjusting the duty cycle while the frequency is kept constant. It has been found that an efficient operation and dc regulation is optimum for a duty cycle between 0.15 and 0.40; for a duty cycle higher than 0.4 the power transfer becomes very low and for duty cycle lower than 0.15 the H bridge loses its soft switching capability [2].

In the simulation model, the dc line current is 2000 A, $C_H = 6 \mu\text{F}$, $C_1 = 500 \mu\text{F}$, the air-core transformer is presented as a mutual inductance with $L_{11} = 100 \mu\text{H}$, $L_{22} = 400 \mu\text{H}$, $M = 120 \mu\text{H}$ and the dc load $R = 160 \Omega$. Without considering the control system, steady state parameters for 20 % duty cycle are shown in Fig. 4 with delivered power 2.3 MW.

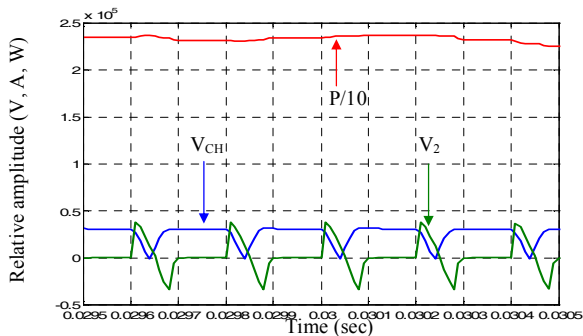


Fig. 4 Static parameters for 20% duty cycle

C. Current-fed inductor-switched converter

This method [7] basically uses the same configuration as B but the switched element is the primary of the isolation transformer (Fig. 5). The main converter is current-sourced line-commutated and the control of firing angle is used to control the dc link voltage. The element L_2 is the commutating reactance for the main converter; C_1 and L_1 constitute a filter for reducing the noise introduced into the main line.

Having to switch very high current, the frequency is low (300-400 Hz) and the control that is done upon the commutation margin which, as shown in [7], depends on the dc voltage across C_2 . Fig. 6 shows the voltage at the input of the insulation transformer in steady-state; the simulation

results are obtained for $I_{dc} = 2000 \text{ A}$, $L_1 = 1.64 \text{ mH}$, $C_2 = 1000 \mu\text{F}$, $V_{dc} = 25 \text{ kV}$, transformer ratio of 1.6 and a load power of 50 MW.

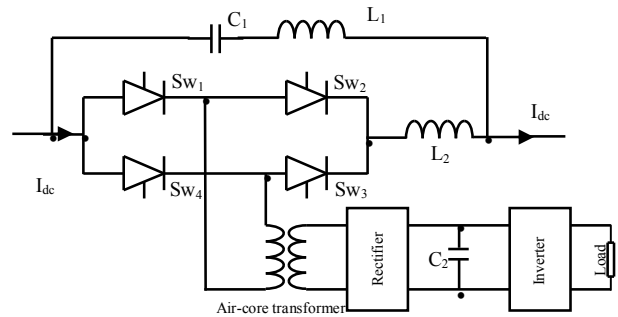


Fig. 5 Current fed inductor switched converter

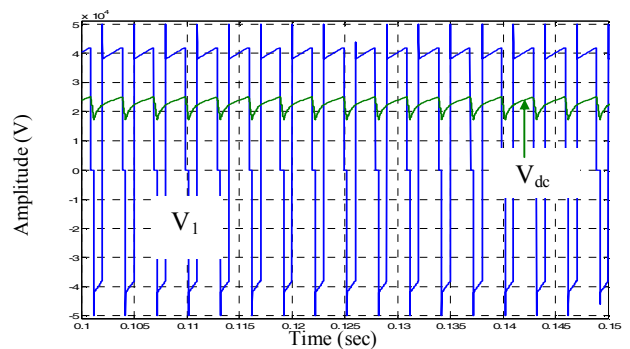


Fig. 6 Steady-state parameters

D. Current-fed PWM chopper

This method [2] consists in inserting in series with the line a chopper which, using PWM switching, charges a capacitor bank thus creating the necessary voltage to supply an inverter (Fig. 7).

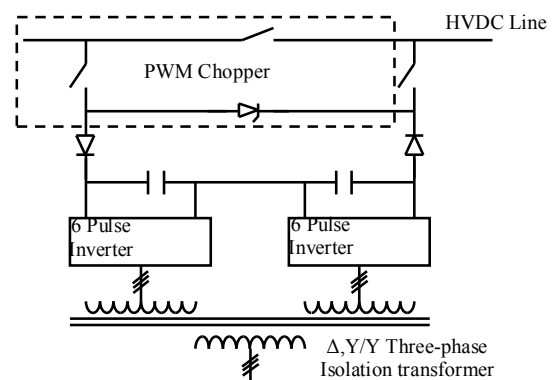


Fig. 7 Current fed PWM chopper

Parameters of the simulation are: switching frequency 5 kHz, charging capacitors of 1000 μF and resistive loads of 10 Ω each. These parameters produce an output power of 10 MW for a duty cycle of 50 % (see Fig. 8).

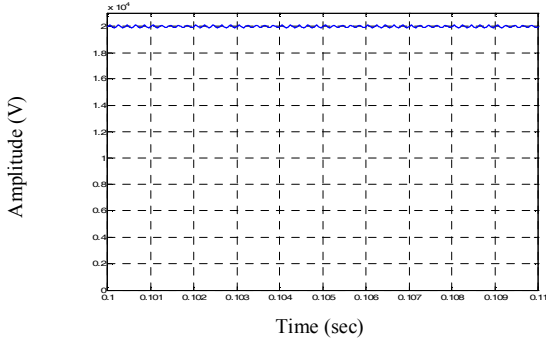


Fig.8 Output dc voltage for 50% duty cycle

III. PROPOSED MODEL AND ANALYSIS

A. Basic Circuit

In Fig. 9 the proposed model is shown. The switching is done using IGBT's connected in a bridge topology; the current transformer is fed with the current flowing through the diagonal of the H topology.

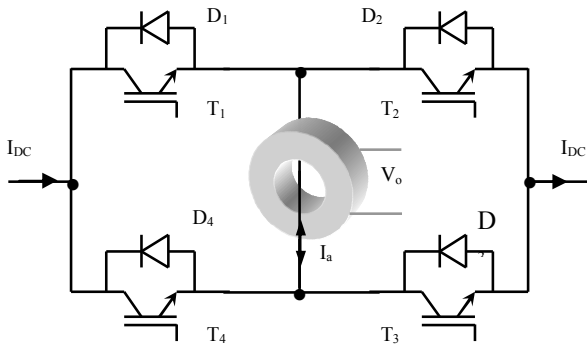


Fig. 9 Proposed model

B. Operation modes

The switching pattern is chosen such that at any moment in time the current flow through main line is not interrupted. The timing analysis of the proposed switching pattern shows four modes:

- ∞ Mode 1: $T_1 = T_3 = \text{ON}$. In this mode the current I_a will flow from T_1 to T_3 .
- ∞ Mode 2: $T_1 = T_2 = T_3 = T_4 = \text{ON}$. In this mode the current I_a will carry on flowing for as short period as decaying inductive current through D_2 and D_4 .
- ∞ Mode 3: $T_2 = T_4 = \text{ON}$. In this mode the current I_a will flow from T_2 to T_4 which is in the opposite direction as in model.

- ∞ Mode 4: $T_1 = T_2 = T_3 = T_4 = \text{ON}$. In this mode the current I_a will carry on flowing for a short as decaying inductive current through D_1 and D_3 .

If the current transformer is represented as a mutual inductance then the four modes could be presented as in Fig. 10.

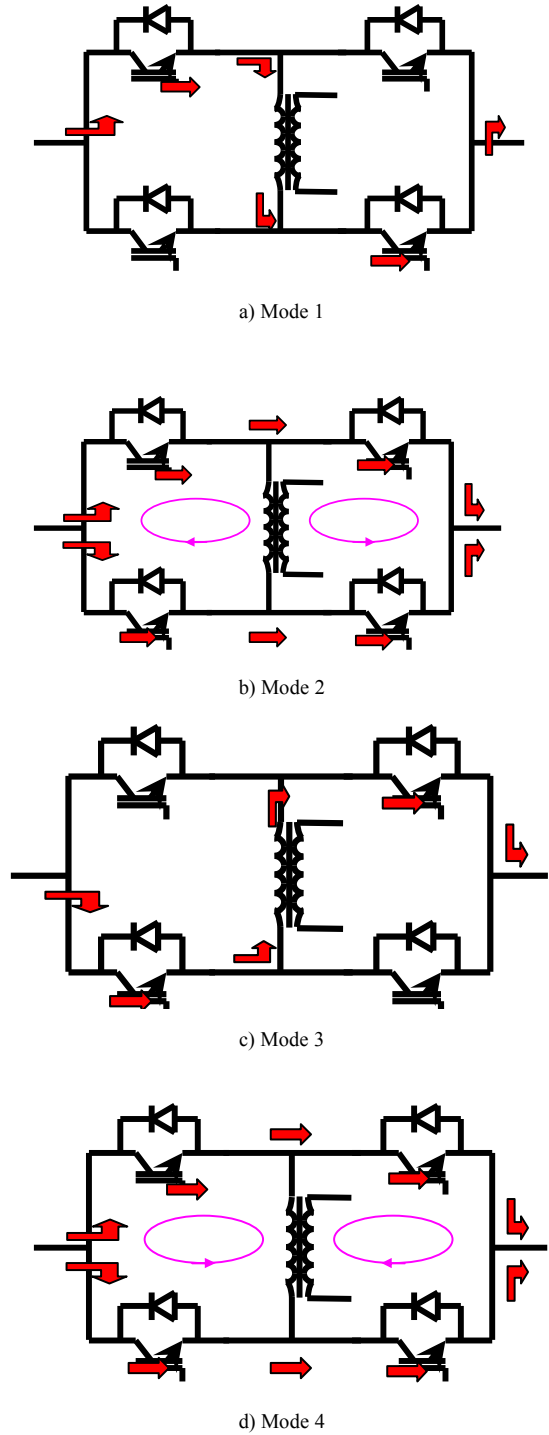


Fig. 10 Operation modes

Once an alternative current has been created, then energy transfer between primary and secondary of the current transformer can be achieved.

It has to be mentioned that in the modes 2 and 4 all switches are ON and thus ensuring the continuity of the main current at any moment in time.

C. Estimation of coupling elements

A current transformer can be seen as the equivalent of two inductors mutually coupled (Fig.11). The elements of the equivalent diagram are:

- ∞ L_1 is the self inductance of the primary: in this situation the main line going through the CT.
- ∞ L_2 is the self inductance of the secondary of the CT: the winding on the CT.
- ∞ L_{12} is the mutual inductance which couples the two inductors.

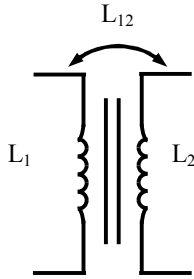


Fig. 11 Mutual coupled inductors

C.1 Primary self inductance

L_1 (the primary) is the inductance of a straight round wire of length l and radius r . The value of L_1 is given by [10]:

$$L = 0.002 \times l \times \left[\ln \frac{2l}{r} - 1 + \alpha_r \times \kappa \right] \quad [\mu H] \quad (1)$$

where:

r = radius of the wire [cm]

l = length of the wire [cm]

μ_r = permeability of the material of the wire

$\kappa = \kappa(\chi)$ a coefficient that depends on χ (frequency and material)

$$\chi = 0.1405 \times (2r) \times \sqrt{\alpha_r \times f / \rho} \quad (2)$$

with f = frequency and ρ = volume resistivity of the wire in micro-ohms centimeter.

C.2 Secondary self inductance

The secondary is an inductance of a toroid with rectangular cross section area. The inductance is given by [10]:

$$L_2 = 0.004606 \times \alpha_r \times n^2 \times h \times \log_{10} (r_2 / r_1) \quad (3)$$

where: n = the number of turns, h = the axial depth of the toroid, r_2 = the external radius and r_1 = the internal radius.

C.2 Secondary self inductance

The mutual inductance between two inductors is given by:

$$L_{12} = \Phi_2 / I_1 \quad (4)$$

In other words it is the ratio between the magnetic flux in the secondary over the primary current. The magnetic flux in the secondary should be determined as a function of the primary current. In order to do this, consider two symmetrical turns in the section with the plane of main conductors crossing the CT as illustrated in Fig. 12.

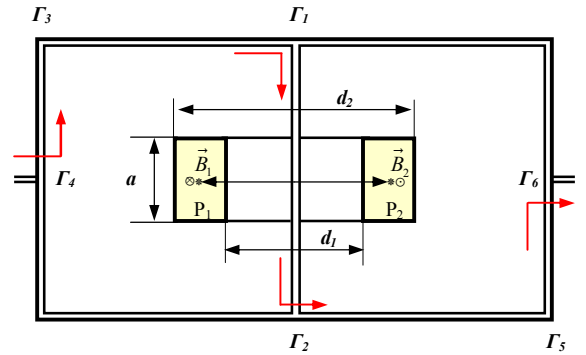


Fig. 12 Cross section through system

In order to clarify the contribution of all the elements of the system to the flux into the secondary, a cross section through the system in the same plane with the main line conductors is shown in Fig. 12. Because the two turns from the cross section are linked, the magnetic flux through them will be algebraically added.

The flux density in the points P_1 and P_2 is influenced by all the current carrying segments: $\overline{\Gamma_4\Gamma_3}$, $\overline{\Gamma_3\Gamma_1}$, $\overline{\Gamma_1\Gamma_2}$, $\overline{\Gamma_2\Gamma_5}$ and $\overline{\Gamma_5\Gamma_6}$. Assuming perfect symmetry and the fact that the two turns are linked, the contributions to the flux density of the segments $\overline{\Gamma_4\Gamma_3}$, $\overline{\Gamma_3\Gamma_1}$, $\overline{\Gamma_2\Gamma_5}$ and $\overline{\Gamma_5\Gamma_6}$ are cancelled therefore:

$$|\vec{B}_1| = |\vec{B}_2| \quad (5)$$

Then, to find the magnetic flux Φ_{12} , it is enough to determine the magnetic flux determined by the current carrying segment $\overline{\Gamma_1\Gamma_2}$ into one turn and then multiply by the number of turns (n). Fig. 13 shows one turn and the current carrying segment $\overline{\Gamma_1\Gamma_2}$.

The magnetic field at a point P created by the current flowing through the conductor l is [11]:

$$H = (I/4\pi x) \cdot (\sin\alpha_2 - \sin\alpha_1) \quad (6)$$

Therefore, the flux density at point P is:

$$B(x, y) = (\mu I / 4\pi x) \cdot (\sin\alpha_2 - \sin\alpha_1)$$

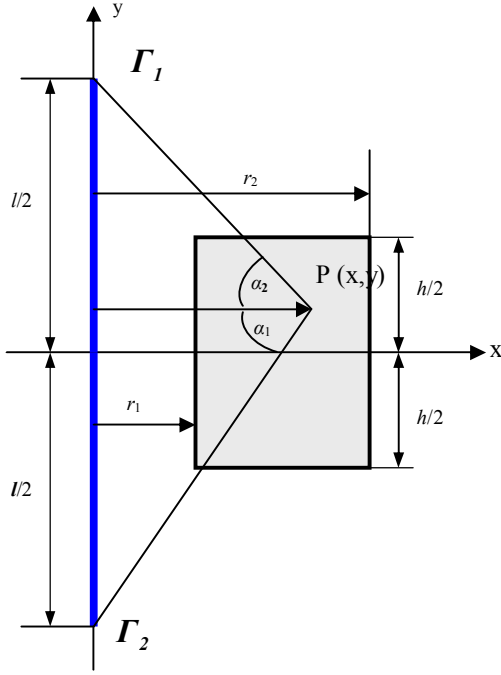


Fig. 13 Flux density at point P

Therefore Φ_{12} is given by:

$$\Phi_{12} = \int_{turn} B(x, y) \cdot ds \quad (8)$$

Completing the mathematics for (8) considering (7) and remembering (4), the mutual inductance is:

$$L_{12} = \frac{\infty}{4\pi} (\zeta_1 - \zeta_2 + \zeta_3 - \zeta_4) \quad (9)$$

where:

$$\zeta_1 = \sqrt{r_2^2 + \left(\frac{l+h}{2}\right)^2} - \sqrt{r_1^2 + \left(\frac{l+h}{2}\right)^2} + \left(\frac{l+h}{2}\right) \cdot \ln \left| \frac{r_2 \cdot \frac{l+h}{2} + \sqrt{r_1^2 + \left(\frac{l+h}{2}\right)^2}}{r_1 \cdot \frac{l+h}{2} + \sqrt{r_2^2 + \left(\frac{l+h}{2}\right)^2}} \right| \quad (10)$$

$$\zeta_2 = \sqrt{r_2^2 + \left(\frac{l-h}{2}\right)^2} - \sqrt{r_1^2 + \left(\frac{l-h}{2}\right)^2} + \left(\frac{l-h}{2}\right) \cdot \ln \left| \frac{r_2 \cdot \frac{l-h}{2} + \sqrt{r_1^2 + \left(\frac{l-h}{2}\right)^2}}{r_1 \cdot \frac{l-h}{2} + \sqrt{r_2^2 + \left(\frac{l-h}{2}\right)^2}} \right| \quad (11)$$

$$\zeta_3 = \sqrt{r_2^2 + (l+h/2)^2} - \sqrt{r_1^2 + (l+h/2)^2} + (l+h/2) \cdot \ln \left| \frac{r_2 \cdot l+h/2 + \sqrt{r_1^2 + (l+h/2)^2}}{r_1 \cdot l+h/2 + \sqrt{r_2^2 + (l+h/2)^2}} \right| \quad (12)$$

$$\zeta_4 = \sqrt{r_2^2 + (l-h/2)^2} - \sqrt{r_1^2 + (l-h/2)^2} + (l-h/2) \cdot \ln \left| \frac{r_2 \cdot l-h/2 + \sqrt{r_1^2 + (l-h/2)^2}}{r_1 \cdot l-h/2 + \sqrt{r_2^2 + (l-h/2)^2}} \right| \quad (13)$$

IV. SIMULATION RESULTS

With the elements of the system estimated and based on a Matlab platform, a simulation model has been created. The simulation parameters were: main dc current 1000 A, the current transformer having winding 1 (the input) of 1 μ H, winding 2 (the output) of 1 mH and mutual inductance of 10 μ H, switching frequency of 1 kHz with a duty cycle of sixty percent and an output load of $R = 50 \Omega$.

Fig. 14 shows the “alternating” current (i_a) and output voltage (v_o) of the current transformer on the given load and with conduction time in each half-cycle of 300 μ sec. The jitter observed is during switching off process, and it is mainly due to decaying inductive current. Fig. 15 shows the voltage across the tap (v_t) and the main current (I_{DC}) which is unaffected.

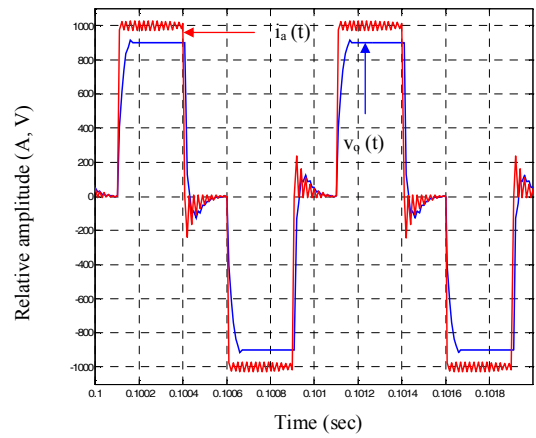


Fig. 14 Waveforms for i_a and v_o

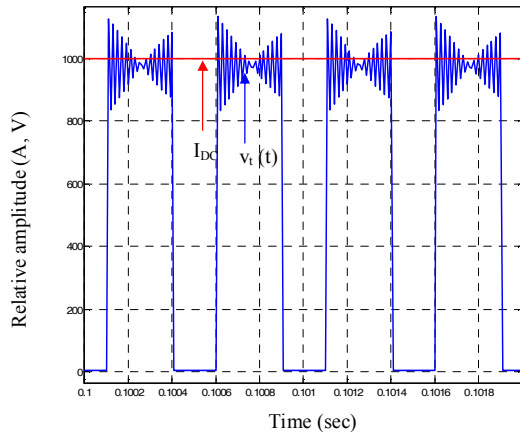


Fig. 15 Influence of the tap

As can be noticed from Fig. 15, for a duty cycle of sixty percent, the rms output voltage is approximately 700 V which represents a power of 10 kW. The influence upon the main current is null and the voltage disturbance is relatively small considering the very high voltage of the HVDC lines.

V. CONCLUSIONS

The present study shows the feasibility of a CT-based direct current source to voltage source converter, eliminating the need for the usual substation in remote areas where small amounts of electric power is needed.

Compared with the methods presented in overview, the proposed method has the advantage of being sure of current continuity at any moment in time.

This method is simple and, with the new development of very powerful IGBTs of above 3000 A, it is practically realizable and relatively easy to implement.

REFERENCES

- [1] U. Lamm, E. Uhlmann, P. Danfors, "Some Aspects of Tapping HVDC Transmission Systems", *DIRECT CURRENT*, Vol. 8, No. 5, May 1963
- [2] M. Bahrman et al., "Integration of small taps into (existing) HVDC links", *IEEE Trans. on Power Delivery*, Vol. 10, No. 3, July 1995, pp. 1699-1706
- [3] V. Collet Billon, J.P. Taisne, V. Arcidiacono, F. Mazzoldi, "The Corsican Tapping from Design to Commissioning Tests of the Third Terminal of the Sardinia-Corsica-Italy HVDC Link", *IEEE Trans. on Power Delivery*, Vol. 4, No. 1, Jan. 1989, pp. 794-9
- [4] M. Bahrman, B. Ekehov, D. McCallum, G. Moreau, J. Primeau, D. Soulier, "Multiterminal Integration of the Nicolet Converter Station into the Quebec - New England Phase II HVDC Transmission System", *CIGRE Proceedings of the 35th Session International Conference on Large High Voltage Electric Systems*, 14 - 103, 1994.
- [5] D.V. Nicolae, "Non-conventional methods for energy extraction from high voltage transmission lines", DTech Thesis, Electrical Engineering Department, Vaal University of Technology, Vanderbijlpark, South Africa
- [6] M. R. Aghaebrahimi and R W Menzies, "Small power tapping from HVDC transmission systems: a novel approach", *IEEE Trans. on Power Delivery*, Vol. 12, No. 4, October 1997, pp. 1698-1703
- [7] A. Ekstrom and P. Lamell, "HVDC tapping station: power tapping from a DC transmission line to a local AC network", *CIGRE Proceedings of 5th International Conference on AC and DC Power Transmission*, London, England, 17-20 September 1991, pp. 126-131
- [8] L. Chetty, N. M. Ijumba and A. C. Britten, *Tapping small amounts of power from HVDC transmission lines using a novel voltage source inverter*, Paper presented at SAUPEC 04, Stellenbosch, South Africa
- [9] M. Aredes, C. Portela and E.H. Watanabe, HVDC tapping using soft switching techniques, *Archiv fur Elektrotechnik*, Volume/Issue 83 1/2, Jan. 2001, pp 33-40.
- [10] Babani, B, *Radio reference handbook*. London: Bernards, 1945.
- [11] Hayt, W H Jr, *Engineering Electromagnetics*. Singapore: McGraw-Hill, 1989.